Comparative Biochemistry and Physiology, Part D 5 (2010) 138–150

Contents lists available at ScienceDirect

Comparative Biochemistry and Physiology, Part D

journal homepage: www.elsevier.com/locate/cbpd

In vivo assessment and potential diagnosis of xenobiotics that perturb the thyroid pathway: Proteomic analysis of *Xenopus laevis* brain tissue following exposure to model T4 inhibitors ☆

Jose Serrano [a,*], LeeAnn Higgins [b,1], Bruce A. Witthuhn [b,1], Lorraine B. Anderson [b,1], Todd Markowski [b], Gary W. Holcombe [a], Patricia A. Kosian [a], Joseph J. Korte [a], Joseph E. Tietge [a], Sigmund J. Degitz [a]

[a] U.S. Environmental Protection Agency, Office of Research and Development, National Health and Environmental Effects Research Laboratory, Mid-Continent Ecology Division, Duluth, MN 55804, USA
[b] University of Minnesota, Department of Biochemistry, Molecular Biology and Biophysics, St Paul, MN 55119, USA

ARTICLE INFO

Article history:
Received 30 December 2009
Received in revised form 24 March 2010
Accepted 25 March 2010
Available online 2 April 2010

Keywords:
2D PAGE
Amphibian
Brain
Endocrine
*i*TRAQ
LC–MS/MS
Proteomics

ABSTRACT

As part of a multi-endpoint systems approach to develop comprehensive methods for assessing endocrine stressors in vertebrates, differential protein profiling was used to investigate expression patterns in the brain of the amphibian model (*Xenopus laevis*) following *in vivo* exposure to a suite of T4 synthesis inhibitors. We specifically address the application of Two Dimensional Polyacrylamide Gel Electrophoresis (2D PAGE), Isobaric Tags for Relative and Absolute Quantitation (*i*TRAQ®) and LC–MS/MS to assess changes in relative protein expression levels. 2D PAGE and *i*TRAQ proved to be effective complementary techniques for distinguishing protein changes in the developing amphibian brain in response to T4 synthesis inhibition. This information served to evaluate the use of distinctive protein profiles as a potential mechanism to screen chemicals for endocrine activity in anurans. Regulatory pathways associated with proteins expressed as a result of chemical effect are reported. To our knowledge, this is also the first account of the anuran larvae brain proteome characterization using proteomic technologies. Correlation of protein changes to other cellular and organism-level responses will aid in the development of a more rapid and cost-effective, non-mammalian screening assay for thyroid axis-disrupting chemicals.

Published by Elsevier Inc.

1. Introduction

It has been long recognized that gene products are differentially expressed in response to stressors, and disease states (Bradley et al., 2003; Kling et al., 2008). Profiling of gene products during chemical exposure facilitates correlation of phenotypic changes directly to quantitative outputs of transcripts, proteins, and metabolites (Villeneuve et al., 2008; Hemmer et al., 2008; Johns et al., 2009; Garcia-Reyero et al., 2009; Koulman et al., 2009). Current state of the research supports the potential of gene product profiling to provide reliable molecular and cellular-level mechanistic data. In ecological risk assessment, 'omic' approaches have been applied to decipher the underlying mechanisms of chemical toxicity with success (Daston et al., 2008; Ankley et al., 2008). For example, proteomics methods have been applied to screen for hepatic responses in zebrafish following exposure to select brominated flame retardants (BFR), and thereby provide molecular information about early responses reflecting potential biomarkers to the adverse effects of BFR exposure (Kling et al., 2008).'Omic' technologies also provide a means for the interrogation of a variety of active biomolecules in a cell or tissue while providing relatively unbiased approaches for mode of action (MOA; for definition and differences with mechanism of action see Borgert et al. (2004) and Ankley et al. (2010)) determination (Edwards and Preston, 2008). Further, the potential of toxicogenomics to promote advances in regulatory ecotoxicology by reducing uncertainty in risk assessment and optimizing the use of continuously shrinking resources has been acknowledged (Ankley et al., 2008). However, assessment of chemically-induced adverse effects by comparing 'omic' signature profiles has been primarily applied to rodent models for extrapolation to human endpoints

Abbreviations[2]: *i*TRAQ®, isobaric tags for relative and absolute quantitation; SCX, strong cation exchange chromatography; LC-qTOF/MS, liquid chromatography-quadrupole-time of flight-mass spectrometry; T4, thyroxine; MET, methimazole; PER, perchlorate; PTU, 6-propylthiouracil; TBP, tributylphosphine; TFA, trifluoroacetic acid; MMTS, methyl-methanethiosulfonate; CHAPS, 3-[(3-cholamidopropyl) dimethylammonio]-1-propanesulfonate; ABC, ammonium bicarbonate; PIC, protease inhibitor cocktail; IPG, immobilized pH gradient strips; IEF, isoelectric focusing; Ups, unused ProtScore; NCBI, national center for biotechnology information; HPT, hypothalamus–pituitary–thyroid gland axis/hypothalamohypophysial-thyroid axis.

☆ This document has been reviewed in accordance with U.S. Environmental Protection Agency policy and approved for publication. Mention of trade names or commercial products does not constitute endorsement or recommendation for use.

* Corresponding author. USEPA/ORD/NHEERL/MED, 6201 Congdon Blvd, Duluth, MN, 55804, USA. Tel.: +1 218 529 5118; fax: +1 218 529 5003.
E-mail address: serrano.jose@epa.gov (J. Serrano).

[1] These authors contributed equally to the manuscript.

[2] Complete protein names and corresponding abbreviations used throughout the text are listed in Tables 1 and 2.

1744-117X/$ – see front matter. Published by Elsevier Inc.
doi:10.1016/j.cbd.2010.03.007

(Ekman et al., 2007). Consequently, much less attention has been provided to the use of 'omic' methods, especially proteomics, for assessing toxicity pathways and adverse outcomes (for definition see NRC, 2007, and Ankley et al., 2010) of environmental stressors in aquatic surroundings or in ecological risk assessment. Current technological and informational limitations in ecotoxicology are more important for endocrine-disrupting chemicals, where there is a critical need to understand both MOA and associated adverse outcomes (Ankley et al., 2010).

Changes in protein patterns are more likely to reflect disturbances in an organism than alterations in other gene products, including changes accompanying alterations in cellular function (Albertsson et al., 2007; Sveinsdottir et al., 2008). However, only a small portion of the proteome is usually identified and quantified in a single experiment even for organisms with complete or near complete genomic sequences. Specifically, molecular profiles, fingerprints, or markers derived from protein differential expression analyses can be identified with state-of-the-art proteomic methods and used as a MOA-specific screening or diagnostic test (Walker et al., 2006; Salinas et al., 2008; Salinas et al., unpublished results; Martyniuk et al., 2009). Yet, the utility of similar approaches for species relevant to ecotoxicology testing remains limited by the lack of the species' gene sequence information and the mass of sample available for analysis. Some studies have targeted the elucidation of signal transduction pathways or characterization of target proteins/peptides in amphibian brain (Gasser and Orchinick, 2006; Pagliato et al., 2006). However, neither the brain proteome composition, nor the brain protein expression patterns produced by exposure to endocrine disrupters have been well investigated in amphibian species. The lack of information has been partially attributed to tissue size limitations in the anuran tadpole. In our studies, brain proteome information is needed to populate a hypothalamus–pituitary–thyroid gland axis (HPT) model capable of integrating data from different levels of biological organization into a coherent system.

The relevance of thyroid axis disruption when evaluating risks associated with chemical exposure has been recently addressed (Tietge et al., 2010). For instance, thyroid hormone (TH) synthesis inhibition is important in the anuran species because it leads to developmental delay. To improve our ability to detect and potentially screen for HPT axis disruption, we applied differential protein profiling to investigate the protein expression patterns produced by a suite of model T4 synthesis inhibitors (Methimazole—MET, Perchlorate—PER, and 6-Propylthiouracil—PTU) in the brain of pro-metamorphic *Xenopus laevis* tadpoles during *in vivo* short-term exposures (0–96 h). The brain is also a key organ target of TH action in vertebrates where disruption of TH action can lead to permanent developmental defects (Helbing et al., 2007a,b). We hypothesized that physiological changes in the brain are reflected in the proteome, and that chemicals inducing TH synthesis inhibition will produce analogous and measureable protein profiles or fingerprints. The search for, identification, examination, and reporting of brain protein expression profiles as a response to T4 synthesis inhibition are specifically discussed in this paper. We also report regulatory pathways associated with proteins differentially expressed in brain. The expression proteomic technologies most suitable for this analysis were two-dimensional polyacrylamide gel electrophoresis (2D PAGE; see Lopez, 2006) and *i*TRAQ (Isobaric Tags for Relative and Absolute Quantitation; Applied Biosystems) labeling in conjunction with 1D or 2D LC–MS/MS. The combination of two-dimensional liquid chromatography (2D LC), stable isotope labeling, and tandem MS (MS/MS) has emerged as one of the standard techniques for high-throughput protein identification and relative quantitation (for review and applications see Ross et al., 2004; Choe et al., 2005; Issaq et al., 2005; Nesvizhskii et al., 2007; Wehr, 2007; Portman et al., 2009; Venkateshwar et al., 2009). *X. laevis* was selected as the target species since an established inventory of thyroid axis endpoints such as gland histology and cell numbers, circulating thyroid hormone (TH) concentrations and thyroidal TH, as well as associated iodo compounds are available (Degitz et al., 2005; Tietge et al., 2005, 2010; Grim et al., 2009). In addition, gene expression data for *X. laevis* exposure to model T4 inhibitors have been reported for brain, tail and hindlimb (Helbing et al., 2007a,b; Part 1 and 2). A challenge for protein characterization of *X. laevis* tissue is that the pseudo-tetraploid organism lacks a fully-sequenced genome. However *X. laevis* duplicated genes are functionally similar and show minimal divergence (Brown et al., 1996).

Therefore as part of a multi-endpoint systems approach to develop methods for studying the adverse effects of endocrine chemicals in vertebrates, the main objective of this investigation was to apply gel-based and non-gel modern proteomic technologies to assess protein composition and relative abundance changes within the developing anuran brain following exposure to model thyroid axis disrupters. A sub-objective was to supply protein regulation information needed to assess and ultimately select candidates representative of toxicant effect with the potential to be used as or to develop diagnostic indicators of thyroid axis disruption (or alternatively for the development of new diagnostic indicator tests). Overall method development addressed challenges associated with: 1) limited amount of brain tissue as well as protein available for analysis, 2) lack of a fully-sequenced genome for *X. laevis*, and 3) the use of pituitary-containing brain as primary target tissue, as opposed to intact pituitary.

2. Materials and methods

2.1. Animal care and in vivo chemical exposure

2.1.1. Animals

X. laevis larvae used for all the studies were obtained from an in-house culture where adults were injected with human chorionic gonadotropin (HCG) to induce reproduction as described by Degitz et al. (2005).

2.1.2. Toxicant solutions

Stock solutions for MET, PER and PTU (Sigma, St. Louis, MO, USA) were prepared by dissolving each chemical in Lake Superior water (LSW). Exposure chemical concentrations for analysis of *X. laevis* brain tissues were 100 mg MET/L (8.8×10^{-4} M), 20 mg PTU/L (1.2×10^{-4} M), 4 mg PER/L (4.8×10^{-5} M), and 0 mg control/L. Toxicant concentrations were selected as they were determined to be maximally effective concentrations based on developmental and histological *in vivo* responses in *X. laevis* (for MET and PTU see Degitz et al. (2005)and for PER see Tietge et al. (2005)). In each experiment, chemical treatments and controls were conducted simultaneously in separate tanks from groups established from the same batch of larvae.

2.1.3. Exposure system

All experiments were conducted in an in-house designed computerized electronic exposure system as described by Tietge et al., 2005. Brain studies were conducted in six tanks of one exposure concentration for each treatment, i.e. MET, PTU, PER and controls.

2.1.4. Water characteristics

Prior to use, LSW was filtered, sterilized with ultraviolet light (Aquionics, KY, USA), and heated to 21 °C. Exposure tanks were immersed in a monitored water bath system to maintain temperature uniformity. Dissolved oxygen and pH were measured weekly on a minimum of twelve exposure tanks. Hardness and alkalinity determinations were made on two tanks (control and high concentration) once during each study. All other water characteristics were measured using methods described by the American Public Health Association (APHA, 1992).

2.2. Chemical analyses

2.2.1. Methimazole and PTU

Water samples collected from the exposure chambers were placed into vials containing methanol, mixed, and immediately analyzed for

MET or PTU as previously described (Degitz et al., 2005). Analyte concentrations were determined using external standard quantitation with 6-point linear calibration curves (4.6×10^{-5}–9.0×10^{-4} M and 3.1×10^{-6}–1.2×10^{-4} M for MET and PTU respectively).

2.2.2. Perchlorate

Water samples were collected from PER exposure chambers, refrigerated for 7 days and then analyzed as described by Jackson et al. (2000) using a Dionex ion chromatography system (Sunnyvale, CA, USA). Analyte concentrations were determined using external standard quantitation with a 6-point linear calibration curve (0–5.0×10^{-5} M).

2.3. Animal exposure

For *X. laevis* brain analyses, 21-day post-fertilization larvae were anesthetized with MS-222 (Sigma; 100 mg/L in $NaHCO_3$), and sorted by stage following Nieuwkoop and Faber's (1994) guidelines. After recovery in LSW, stage 54 tadpoles (3.1 cm/295 mg average) were placed into 12 tanks containing clean LSW water and randomly transferred into 24 exposure tanks (A and B pools for controls and each treatment per exposure time). Mortality observations and dead larvae removal were made daily. Studies were initiated with stage 54 larvae and conducted for 24-, 48-, and 96 h. Larvae mortality did not exceed 1 tadpole (<3%) at any exposure time.

2.4. Brain tissue preparation and protein determination

To help validate biological reliability of measurements, *X. laevis* tadpoles were pooled at random for normal development prior to exposure, and at stage 54 for corresponding chemical treatment and further brain collection. Twenty five brains from control and treated A and B pools at each exposure time (200 per test) were excised into collection buffer (250 mM sucrose,1 mM EDTA, 10 mM Tris–HCl pH 7.9) containing 1% protease inhibitor cocktail (PIC; Sigma-Aldrich). For each brain collected, pituitary attachment to the hypothalamus was visually verified. Brains were preserved on dry ice during collection. Protein extraction and recovery from tissue were optimized with Bio-Rad's ReadyPrep Sequential Extraction Reagent (5 M Urea/ 2 M Thiourea/2% CHAPS/2% SB 3–10/40 mM Tris pH 9.5 plus 0.2% ampholytes; Hercules, CA, USA). Briefly, 85–110 mg of brain tissue per sample pool were disrupted in a microfuge tube containing extraction reagent, PIC and tributylphosphine (TBP; Sigma) using a disposable pestle. Samples were then sonicated on ice (5× at 3 s intervals with 1 s rest interval), incubated with benzonase (5 ng; 30 min at 37 °C; Sigma), and centrifuged at 14,000 *g* for 25 min. Protein content in supernatants was determined by DC Protein assay (Bio-Rad) with albumin standards. Lysate protein concentration was re-determined prior to isoelectric focusing (IEF) and after sample desalting for *i*TRAQ labeling as described below.

2.5. 2D PAGE experiments

Experiments with brain extracts were performed using 75 µg of protein from each sample pools A and B. Samples in Bio-Rad's IEF buffer were loaded onto pH 3–10 and 4–7, 11 cm immobilized pH gradient strips (Ready Strip IPG, Bio-Rad) by active rehydration (50 V; 12 h at 20 °C). Isoelectric focusing was performed at 20 °C in a PROTEAN IEF cell (Bio-Rad) using manufacturer's suggestions. IEF gels were then reduced, followed by cysteine alkylation (25 min each) with Bio-Rad's equilibration buffers I and II respectively. Strips were loaded onto precast Criterion 8–16% gradient gels (Bio-Rad) for electrophoresis. Protein standards (Bio-Rad; Invitrogen) were applied during each gel run to estimate MW. Isoelectric points (pI) were estimated using the pH gradient of the IPG gels. A total of 48 gels per exposure time (3 replicates per chemical plus controls, per sample pool and per IPG pH range to ensure reproducibility) were stained overnight with SYPRO Ruby® (Bio-Rad). Gels were scanned, protein intensity of gel spots was normalized, and data was analyzed with PDQuest™ Version 7.3 software (Bio-Rad). Manual inspection of selected spots was also performed to correct for artifacts in spot editing and/or automatic spot matching. An average of 690, 830, and 838 spots were detected on 96, 48 and 24 h gels respectively. Confirmation of differential protein expression relied upon both multiple gel replicates and multiple treatments showing the same pattern of protein induction. Selection of differentially expressed brain proteins for LC–MS/MS was based on the following criteria: 1) two-fold relative abundance difference for a minimum of two treatments in comparison to controls, 2) *p*-value of <0.05, and 3) coefficient of variance <13% for at least 4 gel replicates as determined from quantification.

2.6. Gel spot excision and preparation for LC–MS

Proteins were aseptically excised from gels with the Genomic Solution ProPic (Genomic Solutions, Ann Arbor MI, USA), and placed into 96 well pierced plates. Tryptic digestion was performed on the Genomic Solution ProPrep. Peptide preparation for MS analyses was performed following a modification of the method reported by Shevchenko (1996). Briefly, gel slices were subjected to two series of dehydration and hydration steps by addition, incubation with, and removal of acetonitrile (ACN) and ammonium bicarbonate (ABC; 25 mM; Sigma). Protein in gel slices was reduced by incubation with 10 mM DTT/25 mM ABC (30 min at 60 °C). The DTT solution was aspirated, immediately replaced with 55 mM iodacetamide/25 mM ABC, and incubated for 30 min at 25 °C. The iodoacetamide solution was aspirated, followed by dehydration and hydration steps as above. Trypsin (sequencing grade; Promega, Madison, WI, USA; at 12 ng/µL in 25 mM ABC/5 mM calcium chloride) was added and gel slices were incubated for 10 h at 37 °C. The reaction was terminated with formic acid to a final 0.1% v/v. Gel slices were subjected to multiple extractions with ACN followed by addition of 0.1% formic acid (10 min with each reagent). Solutions from a single plug were pooled, frozen, and concentrated in a speed vacuum (Savant Instruments, Ramsey, MN, USA). Samples were rehydrated in appropriate buffer for 1D LC–MS.

2.7. Sample preparation for iTRAQ-peptide labeling experiments

Aliquots of brain protein lysate from samples analyzed by 2D PAGE (60 µg) were incubated with 1.14 M NaCl (15 min; 37 °C) to remove ampholytes and PIC. Samples were concentrated by centrifugation (5000 *g*; ~100 µL) using an Amicon Microcon YM-3 filter (Millipore, Bedford, MA), and the process was repeated with 125 µL of NaCl. Salt was removed by two additional centrifugation steps with 150 µL nanopure water to a final sample volume of 80–100 µL. Protein concentration after sample desalting was verified with Bradford reagent by absorbance measurements at 590 nm.

2.8. Proteolytic digests and peptide labeling strategy for iTRAQ analyses

The *i*TRAQ approach for peptide labeling has been described in the literature (Ross et al., 2004; Lin et al., 2006). For *i*TRAQ experiments, confirmation of differential protein expression relied mostly upon multiple treatments showing the same pattern of protein induction due to limited sample availability after gel experiments (see below). As such, multiple chemicals were used to compensate for a low number of technical replicates analyzed. Differential expression was validated only for proteins exhibiting the same overall response for at least two of the inhibitors in comparison with controls (see Section 2.13 for protein report criteria used). Specifically, equal amounts of brain protein from control and treated *X. laevis* brain samples were labeled with *i*TRAQ reagents (Applied Biosystems (AB),

Foster City, CA, USA) according to the manufacturer's protocol. However, the amount of brain protein needed for gel replication and for optimization of *i*TRAQ experiments resulted in insufficient amounts of protein available for peptide labeling of individual pools. Therefore, with the exception of control pools, low protein extract concentrations required pooling of the 96 h samples into a single aliquot prior to labeling. Controls were also pooled for *i*TRAQ experiments. Forty-eight hour sample pools were also combined, but sufficient material was available for duplicate labeling. Briefly, isobaric peptide labeling was performed with the 4-plex *i*TRAQ chemical tags as follows: protein samples were denatured, reduced, cysteine's residues modified with methyl-methanethiosulfonate (MMTS; Sigma), and subjected to tryptic digestion. Samples were then labeled as: Control = 114, PTU = 115, PER = 116 and MET = 117. In addition, the same amount of control sample pools A and B were labeled with different tags (114 and 115) at 48 and 96 h prior to pool mixing for protein content and abundance comparison (internal controls analysis). Average ratios for identified proteins in duplicate controls (control:control) at each exposure time point were calculated. A representative 48 h treated pool sample set (MET) was also labeled and analyzed in duplicate as done for control pools. Labeled samples from each representative experiment were combined and dried in a speed vacuum. All samples were applied to a SepPak $_{C18}$ (Waters Corporation, Milford, MA, USA) cartridge for partial purification and vacuum-dried prior to 2D LC–MS/MS analyses.

2.9. 1D LC–MS/MS parameters of gel digests

Peptides were separated by capillary HPLC (Moseley et al., 1991) using homemade fritless columns (Gatlin et al., 1998). The LC system (LC Packings/Dionex, Sunnyvale, CA, USA), was on-line with an AB QSTAR Pulsar *i* quadrupole-TOF MS instrument (Foster City, CA, USA), which was equipped with Protana's (Denmark) nanoelectrospray source. Experimental LC and MS parameters were used as previously published (Kapphahn et al., 2003) with the exception of the gradient elution parameters. Specifically, samples were loaded on to the trap cartridge and washed for 17 min at 35 µL/min using load buffer (98:2, water:ACN mixture and 0.1% formic acid); followed with a linear elution gradient from the analytical C18 capillary column at 0–35% ACN over 45 min, 35–80% ACN over 2 min, 80% ACN for 10 min and, column re-equilibration 80–0% ACN over 0.2 min to a final equilibration of 10 min in load buffer.

2.10. 2D LC–MS/MS parameters for brain lysates

Labeled brain peptides were subjected to fractionation (10 aliquots) by strong cation exchange (SCX) liquid chromatography as described by Lund et al. (2007). Fractions were collected at 3 min intervals and those showing a 280 nm absorbance >2.0 mAU were dried *in vacuo* for reversed phase LC. Second dimension reversed phase LC separation was identical to 1D analysis (described above).

2.11. Database searches

Tandem mass spectra from *i*TRAQ experiments were analyzed with ProteinPilot™ version 2.0 software (AB). The Paragon™ scoring algorithm optimizes sequence coverage for identification of atypical peptides without increasing the false positive rate or analysis time (Shilov et al., 2007). Peptide MS/MS data provided protein identifications, and the ratios of the relative intensities of reporter (chemical tag) ions (114–117 *m/z*; 40 counts minimum) provided relative protein abundance among indicated sample types. Search parameters were as follows: MMTS, trypsin, urea denaturation (as a special factor), thorough search mode (includes semi-trypsin peptides), biological modifications (includes more than 220 post-translational and artifactual modifications), and amino acid substitutions. The protein database (DB) was a subset of the September 2008 nrNCBI protein DB (ftp://ftp.ncbi.nih.gov/blast/db/FASTA) containing human, mouse, rat, fish and amphibian entries (hmrfac) plus 179 common contaminants (553,072 total proteins). False positive rates of assignment for protein identification were estimated using the method reported by Elias et al. (2005) and found to range between 0 and 0.43% for all treatments. The composite DB created for this purpose (target plus decoy hmrfac DB; September, 2008) contained 1,106,144 protein entries. Gel protein searches were performed with ProteinPilot™ version 1.0.4 and the April 2008 NCBIhmrfac DB (489,862 entries). Search parameters included cysteine alkylation with iodoacetamide; all other parameters were identical to *i*TRAQ search parameters. Manual examination was also performed to assist in protein identification confidence across species. Tandem mass spectra were extracted, but charge state deconvolution and deisotoping were not performed. All MS/MS data were analyzed using Mascot (Matrix Science, London, UK; Version 2.2.03; www.matrixscience.com; Perkins et al., 1999) and X! Tandem (www.thegpm.org; Version 2007.01.01.1; Craig and Beavis, 2004). Both X! Tandem and Mascot searches were performed with the Sept 2008 hmrfac DB and trypsin as the digestion enzyme. Search parameters included fragment ion mass tolerance of 0.60 Da and precursor ion mass tolerance of 0.20 Da. Oxidation of methionines, cysteine-MMTS and *i*TRAQ labeled lysines and N-termini were set as variable modifications for both search engines. Criteria used for protein identification were as follows: Scaffold software (version 02_01_00, Proteome Software Inc., Portland, OR, USA) was used to validate MS/MS-based peptide and protein identifications as described in manufacturer's guidelines. Peptide identifications were accepted at greater than 90% probability as specified by the Peptide Prophet algorithm (Keller et al., 2002; www.proteomecenter.org/software.php). Protein identifications were accepted at greater than 90% protein probability and inclusion of at least 2 identified peptides. Protein probabilities were assigned by the Protein Prophet algorithm (Nesvizhskii et al., 2003; Nesvizhskii and Aebersold, 2005). Proteins that contained similar peptides and could not be differentiated based on MS/MS analysis alone were grouped to satisfy parsimony principles.

2.12. Criteria for inclusion of peptides identified by ProteinPilot™-MS data

Protein candidates and identifications reported from ProteinPilot™ include all peptides with >1% confidence (a Paragon scoring parameter) except in cases when amino acid substitutions or biological modifications (e.g., PTM's) were present, in which cases <99% confidence peptides were excluded. Peptides used for quantitation by *i*TRAQ were filtered. Peptide ratios with >25% error (a ProteinPilot™ statistic; see software Help documentation) were eliminated from average ratio determinations. Criteria were chosen manually and based on the presence of weak S/N for reporter ions. Second, in cases when product ions originate from >1 peptide (as judged by visual inspection of precursor mass spectrum), the peptides were removed from the average protein *i*TRAQ ratio calculation. Peptides were filtered from proteins in ProteinPilot™ software and new statistical parameters were generated in the software.

2.13. Data reporting and MS protein reporting from ProteinPilot™

Assessment of *X. laevis* brain proteome coverage after electrophoresis and peptide tagging experiments was performed by inspection of the MW and pI range of proteins identified at 96 and 48 h. Protein sub-cellular location, biological process, molecular function, estimated MW/pI and other relevant data for brain expressed proteins was obtained from the latest NCBI, Universal Protein (UniProt), Celera Discovery System (CDS), and Panther information resources. Regulatory pathways associated with expressed proteins were obtained

from the Kyoto Encyclopedia of Genes and Genomes (KEGG; Kanehisa and Goto, 2000; www.genome.jp). All protein ratios were reported with bias correction invoked (within ProteinPilot™ software; see Kassie et al., 2008). Significant protein *i*TRAQ ratios reported met the following criteria: 1) fold change direction for a minimum of two T4 inhibitors were in agreement; 2) a minimum of two peptides for identification and three peptides for relative quantitation; 3) p-value <0.05 for average *i*TRAQ ratio, 4) protein error factor (EF) <2, and 5) changes were supported by independent labeling of internal controls and treated pools. Fold change (average protein ratio relative to controls) was obtained from the protein spectra as suggested by the manufacturer and is included with the Supplemental information. The EF is a measure of how well a mean protein ratio was determined (a reflection of the variance and the number of peptide measurements), and is used to calculate the 95% confidence interval (CI) of the average *i*TRAQ ratio for each protein [EF = 95% CI, where 95% CI range = (ratio × EF) − (ratio / EF)]. Protein relative abundances were reported as an average ratio with the specific 95% confidence interval (avg ratio [95% CI]; see ProteinPilot™ 2.0 Online Help). The Unused ProtScore (Ups) is a ProGroup™ parameter, more specifically a measurement of all the peptide evidence for a protein that is not attributed to a higher ranking protein. Therefore it is the best indicator of protein confidence. For example, at 95% confidence level (Ups = 1.3), there is a false positive identification chance of about 5% (see Ernoult et al., 2008). A protein competitor error margin of 2.0 (99%) was used for all analyses. In some cases, response to two or more chemicals indicated a statistically significant increased or decreased relative abundance ratio for a protein, but the internal control samples showed the same outcome for the same protein (control:control p-value <0.05) at the corresponding exposure time. The proteins in this subset were not reported in Table 1.

3. Results

3.1. Brain protein characterization by 2D PAGE followed by 1D LC–MS

Combination of electrophoresis and MS methods provided the means for effective separation, detection, quantitation, and identification (selected spots) of *X. laevis* brain proteins in the ranges of 9–100 kDa and 3.0–9.8 pI. Overall, 19 and 10 spots at 96 and 48 h, respectively, showed a significant change in relative abundance and were analyzed by LC–MS/MS (Table 1). Figure A-Supplemental displays histograms correlating 2D PAGE normalized average spot intensity to MET, PER, and PTU exposure for differentially expressed *X. laevis* proteins in intact brain extracts at 48 and 96 h. Significant differences in relative abundance levels between treated and control samples were not found at 24 h of exposure. This finding correlates well with the lack of significant gene regulation observed in the larvae brain by at least 2 of the target chemicals after *in vivo* exposure for 24 h (unpublished data; NHEERL-Duluth), and supports the minimum selection criteria proposed in this study for selection of differential expression requirements.

Nine and six proteins showed increased relative expression levels (upregulation) compared to controls at 96 and 48 h after exposure, respectively (see Table 1 and Fig. 1). Likewise, 10 and 4 proteins showed decreased relative expression levels (downregulation), respectively. Significant changes corresponding to treatment with the three chemicals were observed in 8 and 7 of the detected proteins relative to controls at 96 and 48 h, respectively. These proteins were identified as Tpi, Hnrpk, Flot1c, alpha fodrin, Xac1, eno1, LOC397751, Cct6a at 96 h, and Hnrpk, Hsc70, LOC494650, Mdh2a, MGC84000, Cct5 and Capzb at 48 h. Average fold change among expressed proteins was 3.0 and 2.6 at 96 and 48 h respectively. The highest average fold change in abundance compared to controls was shown by Tpi and LOC494650. Experimental MW and pI for expressed proteins were within 10% of theoretical values for all proteins except for fodrin alpha (brain spectrin; Spot 4) and Tubb5 (Spot G7), suggesting truncation or modification to these proteins. Excision of protein spots with low densities resulted in detection of only a few proteins by MS. Protein abundances for these spots were likely below the detection limit of MS (typically lower than gel staining), after processing by excision and proteolytic digestion (Sriyam et al., 2007).

3.2. Brain protein characterization by iTRAQ isobaric peptide labeling followed by 2D LC–MS

To show the efficacy of labeling, the number of non-*i*TRAQ labeled peptides was counted after 2D LC–MS/MS. Mascot/X!Tandem and ProteinPilot™ searches revealed no peptides without *i*TRAQ labels. A comparison was also made between independently labeled treatment regimes that were expected to show little or no difference. Specifically, an assessment of internal control pools labeled at both 96 and 48 h and two independently labeled MET (48 h) sample pools resulted in a small (less than 1.2% average) number of proteins with significant changes in relative abundance levels between pools A and B, thereby confirming the efficacy of the *i*TRAQ quantitative method. However, the results also suggest that false positives representing expression differences between two equal treatments may occur at a low level in the experiment, thereby making comparison between labeled samples an important step for confirming differential regulation. Table 2 summarizes *i*TRAQ results for proteins differentially expressed by two or more chemicals at 96 and 48 h.

A total of 437 and 612 proteins were identified with >99 and >95% confidence in the 96 h experiment (see Supplemental information for complete data). Twenty-one proteins with an assigned protein confidence of ≥99% were differentially expressed at 96 h by *i*TRAQ labeling when compared to controls. The p-value associated with *i*TRAQ ratio and Genbank identifier (accession number) for proteins differentially expressed at 96 h by a minimum of two inhibitors is presented in Fig. 2. Data show that >75% (49/63) of all p-values reported in the output indicate significance (<0.05). Six of the proteins exhibited significant changes for treatment with all three chemicals. Specifically, Hsp90b, An2/LOC397732, Atp1a3, and Tuba1 showed decreased relative abundance levels by all the chemicals. Triosephosphate isomerase (Tpi) and Nsep1 showed increased relative abundance levels by all chemicals. In the 48 h experiment, 708 and 703 proteins were identified with >99% confidence for replicates 1 and 2, respectively. However, only 2 proteins (Hsp90b and LOC496060), were differentially expressed by multiple chemicals in both replicates with *i*TRAQ technology. The limited number of proteins differentially expressed at 48 h exposures also correlates with an overall lower level of significant gene regulation in the *X. laevis* brain by 2 or more chemicals observed at 48 h in comparison with 96 or 144 h (unpublished data; NHEERL-Duluth). Fig. 3 displays *i*TRAQ ratios that differ from unity for proteins identified in brain extracts at both 96 and 48 h and listed in Tables 1 and 2. Although ratios of treated to control proteins are small, the associated p-values ($p<0.05$) indicate that the changes are significant.

As expected, a larger number of proteins within a broader range of MW and pI values from the total detected and validated were characterized with *i*TRAQ tags as compared to 2D PAGE. For differentially expressed proteins reported from *i*TRAQ and electrophoresis experiments, the estimated MW ranged between 5.1–112.7 and 18–91 kDa, respectively. Estimated pI range was from 4.09–10.32 for iTRAQ and 4.6–8.5 for 2D PAGE. Sub-cellular location distribution for differentially expressed proteins was similar for 2D PAGE and *i*TRAQ. Combined data were: membrane (24%), nuclear (24%), mitochondrial (10%), structural (19%), and other (24%). Intact brain analysis by *i*TRAQ labeling showed a variety of membrane and nuclear proteins among the identified components (8.9 and 7.3% respectively at 96 h; 8.4 and 7.1% respectively at 48 h), an observation consistent with the sample preparation methods used to improve isolation of

Table 1
Summary of 2D PAGE results for differentially expressed *Xenopus laevis* brain proteins.

[a]Accession (gi|)	Label in Fig. 1	Species	Protein name and abbreviation	[b]96 h 2D PAGE	[b]48 h 2D PAGE	[c]Average fold change	[d]Predicted and observed MW/pI match for excised proteins (±10%)	[e]Main molecular function
18088719 148232158	G7	*Homo sapiens* *Xenopus laevis*	[f]Tubb protein/tubulin beta chain/Tubb5 (tubulin beta 5 chain)/MGC53125	DR (2)		(−)2.23	NM	Structural molecule and GTPase activity
147901918 27503418	12	*Xenopus laevis*	Ckb protein (creatine kinase brain)/ MGC53426	UR (2)		(+)4.18	M	Kinase, catalytic and transferase activity
148236351 28461382	13	*Xenopus laevis*	Tpi protein (triosephosphate isomerase)/MGC52638	UR (3)		(+)4.21	M	Isomerase, transferase and catalytic activity
147903924 27882469	5,14	*Xenopus laevis*	Hnrpk protein (heterogeneous nuclear ribonucleoprotein K)/MGC53459	DR (3)	DR (3)	(−)3.15/3.07	M	RNA and protein binding; Splicing
51968292 82198772	2,18	*Xenopus laevis*	20 S proteasome alpha 5 subunit/ MGC80760	UR (2)	UR (2)	(+)2.55/2.04	M	RNA, ATP and protein binding; endopeptidase and hydrolase activity
148223071 27448109 27448107	1	*Xenopus laevis*	SNAP-25 protein (synaptosomal-associated protein of 25 kDa)/ MGC68863	UR (2)		(+)3.24	M	Synaptic transmission; SNARE and protein binding
2895520 34783865	3	*Xenopus laevis*	14–3–3 Protein z/MGC64423	DR (2)		(−)3.72	M	Protein domain specific-, DNA and actin binding; transcription activator activity
147902024 26985229	G5	*Xenopus laevis*	Flot1c (flotillin 1C)/MGC132244	DR (3)		(−)3.26	M	Protein binding; lipid raft and structural molecule activity
3122041 28422343	6	*Xenopus laevis*	Dpys13 protein/DRP3 (dehydropyrimidase-related protein 3a)/nsp1 (neural specific protein 1)	UR (2)		(+)3.13	M	Hydrolase, transferase and dihydropyrimidase activity
55663121 929912	4	*Homo sapiens* *Xenopus laevis*	[f]Fodrin alpha chain/spectrin alpha chain brain (fragment) *Xenopus* alpha fodrin 1	DR (3)		(−)2.70	NM (fragment)	Calcium ion, calmodulin, protein and actin binding
148232082 27881811	7	*Xenopus laevis*	Xac1 (cofilin-1a)	DR (3)		(−)3.86	M	Actin and protein binding
148235689 32450571	8	*Xenopus laevis*	Eno1 protein (enolase1 alpha enolase 1)	DR (3)		(−)2.76	M	Transferase, lyase and Mg ion binding activity
147900728 47938744	G1	*Xenopus laevis*	LOC397751 protein (ribonucleoprotein A1a)	DR (3)		(−)3.74	M	Nucleic Acid and protein binding; transcription activator activity
148226082 3928511	G2	*Xenopus laevis*	Aldolase C-brain (aldolase C, fructose biphosphate)	UR (2)		(+)2.79	M	Fructose-bisphosphate, catalytic and lyase activity
147906703 27370850	10	*Xenopus laevis*	Hspa5 protein/BiP/MGC52648/ heat shock 70 kDa protein5 (glucose-regulated protein 78 kDa)	DR (2)		(−)2.06	M	ATP, protein and nucleotide binding; signal transduction activity
54020867 28422362	11	*Xenopus tropicalis* *Xenopus laevis*	Vcp (valosin-containing protein) [f]Vcp/MGC52611/Transitional endoplasmic reticulum ATPase	DR (2)		(−)3.19	M	ATP, lipid, protein, DNA and nucleotide binding
1107470 27696268	9	*Xenopus laevis*	XNIF (low molecular weight neuronal intermediate filament) Ina B-prov/MGC53005	UR (2)		(+)2.21	M	Structural molecule activity; signal transduction and receptor activity
89271999 148233826	24	*Xenopus tropicalis* *Xenopus laevis*	[f]Cct6a (chaperonin containing TCP1 6A zeta 1) MGC81949	UR (3)		(+)2.79	M	ATP, protein and nucleotide binding; hydrolase ATPase and transferase activity
33417138	25	*Xenopus laevis*	Ddah1-prov (dimethylarginine dimethylaminohydrolase 1)	UR (2)		(+)2.63	M	Protein and metal ion binding; hydrolase, transferase and catalytic activity
148222597 27371247	23	*Xenopus laevis*	Hsc70 protein (heat shock cognate protein 70)/MGC52655		DR (3)	(−)2.01	M	ATP and nucleotide binding; chaperone hsc activity
148231542 52138897	15	*Xenopus laevis*	LOC494650 protein (dihydropyrimidinase-related protein 3b)		UR (3)	(+)3.94	M	Hydrolase and transferase activity; protein binding
76780392 147899037	16	*Xenopus laevis*	Mdh2a protein (mitochondrial malate dehydrogenase 2a)/MGC132376		UR (3)	(+)2.26	M	Oxidoreductase and dehydrogenase activity
148236454 49257618	17	*Xenopus laevis*	MGC84000 (guanine nucleotide-binding protein, beta; G protein beta subunit)		UR (3)	(+)2.27	M	Protein binding and signal transduction activity
147902934 29351607	19	*Xenopus laevis*	Uqcrc1 (ubiquinol cytochrome c reductase core protein 1)/ MGC53748 protein		UR (2)	(+)2.37	M	Mitochondrial metalloendopeptidase-, catalytic and metal ion binding activity
148238173 27370869	20	*Xenopus laevis*	Capzb protein (actin-capping protein beta 1)/MGC52754		DR (3)	(−)2.75	M	Actin and protein binding
147906092 28278093	21	*Xenopus laevis*	Fubp1 protein (far upstream element binding protein/FUSE)/MGC53183		DR (2)	(−)3.32	M	Nucleic acid binding and transcription factor activity
148237440 27924333	22	*Xenopus laevis*	Cct5 protein (chaperonin containing TCP1, subunit 5 epsilon)/MGC53061		UR (3)	(+)2.76	M	ATP, protein and nucleotide binding; hydrolase ATPase and transferase activity

[a] Accession numbers in Tables 1 and 2 are NCBI protein accessions.
[b] Observed response in Tables 1 and 2 (number of chemicals triggering response); UR/DR: up- or down-regulation; NC: no change.
[c] Average fold change for proteins in gel experiments (≥2.0) was calculated from individual protein fold changes (≥1.8) relative to controls for at least two T4 inhibitors.
[d] M/NM: match or no match.
[e] When available, the main molecular function and associated pathway(s) for the proteins listed in Tables 1, 2 or 3 were assigned using the latest version of NCBI, UniProt, Celera Discovery System, Panther and PIR/KEGG information resources.
[f] Cases in Tables 1 and 2 where the top winner reported is from a species different than *Xenopus laevis*, and BLAST search using total protein sequence to determine % identity to *X. laevis* was performed. See Supplemental information for footnote (f) to Table 1.

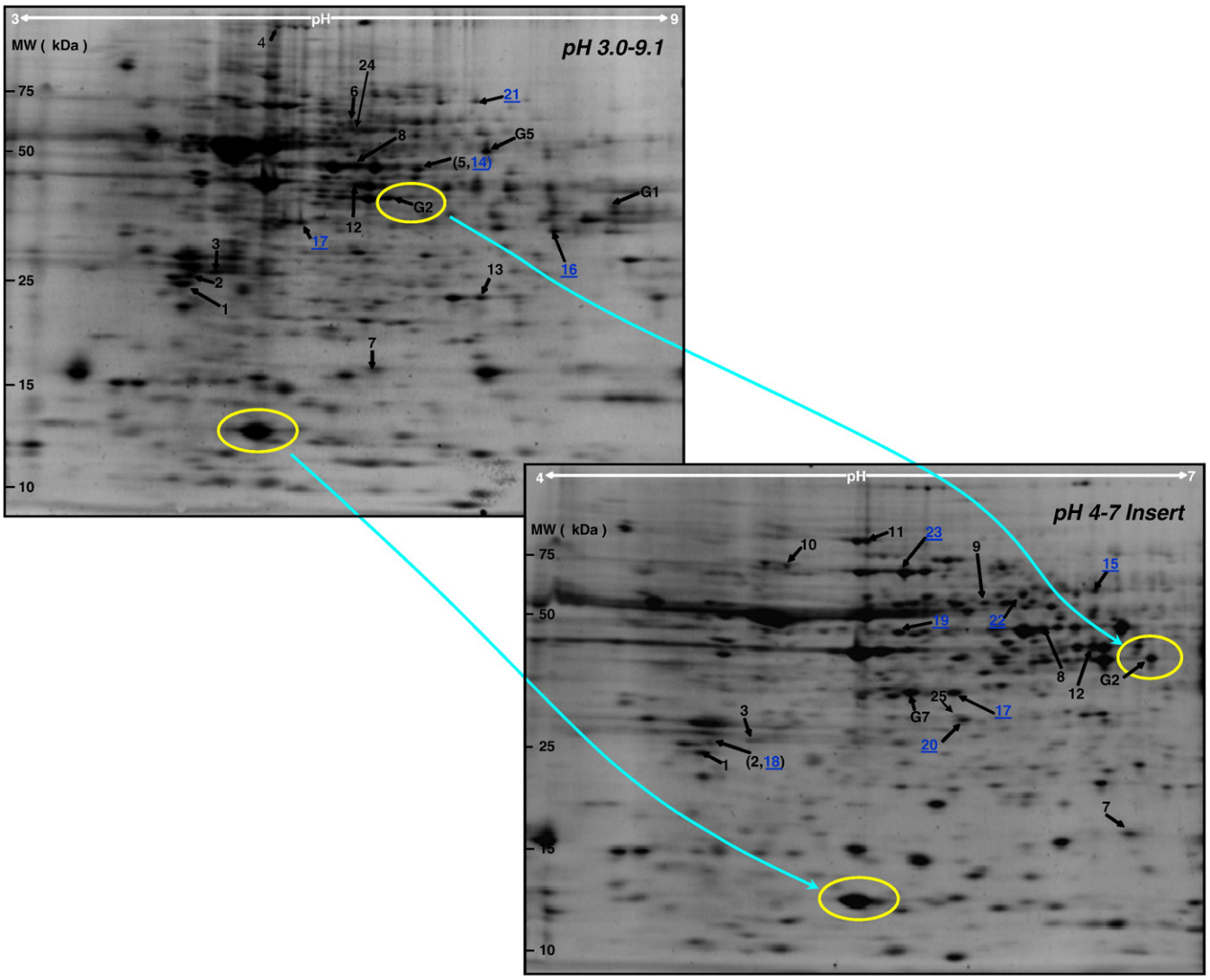

Fig. 1. Representative 2D-electrophoresis reference gels of *Xenopus laevis* intact brain extracts. Relative location of differentially expressed proteins after larvae exposure to T4 inhibitors at 96 (black) and 48 h (blue; underlined) is indicated with an arrow. Lysates were resolved by 2D PAGE, gels were stained with SYPRO Ruby and proteins showing a significant change in average relative abundance levels as compared to controls (≥2.0 fold; see Table 1) were excised for identification by 1D LC–MS/MS. Representative protein profiles are displayed for pH (strip) 3–9.1 (1a) and 4–7 (1b; insert). A total of 27 proteins differentially expressed by at least 2 of the inhibitors were identified. Spot identification is provided in Table 1.

less soluble proteins. A majority of the proteins differentially expressed in gel experiments were also identified in *i*TRAQ experiments (19/27). However, while quantitation of proteins with post-translational modifications is feasible by 2D PAGE, *i*TRAQ labeling will generate paired peptides only for unmodified fragments thus preventing effective quantitation of a modified protein. With the exception of Tpi, factors including lower number of peptides used for quantitation and/or low intensity of reporter ions prevented the unbiased quantitation of the remaining proteins for comparison with gel data. Associated and potential regulatory pathways for differentially expressed brain proteins are listed in Table 3 (see Discussion).

3.3. False positive rates for protein identification and data validation

In ecotoxicogenomics, the use of multi-endpoint and screening methods to assess biological effects results in a large number of potential responses for evaluation, which in turn increases the risk for reporting false positives. Two-dimensional gel data has often been validated by comparison of relative expression levels and identification results for identical proteins during an initial test-set to a larger validation-set (Albertsson et al., 2007). The limited sample availability did not permit the use of a larger sample-set to validate findings obtained with the experimental set in our 2D PAGE studies, but support information such as MW and pI, as well as literature reviews provided means for validation. False positive rates for protein identification were calculated in the shotgun *i*TRAQ experiments using a target/decoy database strategy (Balgley and Laudeman, 2007), providing an estimate on false discovery rates. For proteins with 99% confidence as determined by labeling data, peptide-level false positive discovery rates (%) calculated for each individual file searched were as follows: 96 h (0), 96 h Control (<0.43), 48 h Pool A (<0.027), 48 h Pool B (<0.028), and 48 h Controls (<0.10); see Supplemental. Accepted values for some proteomic platforms have been discussed by Elias et al. (2005).

Comparison of labeled peptides from brain control pools at 96 and 48 h (internal controls) and from a representative 48 h treated pool sample set was also performed to help minimize false positives. Due to the need to pool protein from multiple samples for *i*TRAQ studies, we hypothesized that a lack of significant variability in relative protein abundance levels between individual sample pools (A and B) would also result in minimum protein abundance differences found if the individual sample pools were compared to combined pools and/or

Table 2
Summary of iTRAQ results for differentially expressed *Xenopus laevis* brain proteins.

[a]Accession (gi|)	Species	Protein name and abbreviation	[b]96h iTRAQ	[b]48h iTRAQ (Replicate 1/ Replicate 2)	[c]Average fold change	[e]Main molecular function
148236351 28461382	*Xenopus laevis*	Tpi protein (triosephosphate isomerase)/ MGC52638	UR(3)		(+)1.16	Isomerase, transferease and catalytic activity
148232054 54873686	*Xenopus laevis*	Hsp90beta (heat shock 90 kDa protein beta)	DR(3)	UR(3)/UR(2)	(−)1.23/(+) 1.19/1.12	ATP and unfolded protein binding; chaperone protein activity
148231458 32450058	*Xenopus laevis*	Stmn1 protein (stathmin)/MGC64272	UR(2)		(+)1.19	Signal transducer activity; environmental information processing
148231177 27735427	*Xenopus laevis*	hypothetical protein LOC398459 (cytoplasmic beta actin)/MGC52661	DR(2)		(−)1.15	ATP, nucleotide and protein binding; structural molecule activity
50925070 82235567	*Xenopus laevis*	Xtp protein (microtubule-associated protein)/ Unknown (protein for MGC:86289)	UR(2)		(+)1.11	Cytoskeletal regulatory protein binding Microtubule-associated processes
148232076 76780386	*Xenopus laevis*	[h]hypothetical protein LOC734877/MGC132184	UR(2)		(+)1.22	Unclassified
148222322 51703543	*Xenopus laevis*	[h]MGC84072	UR(2)		(+)1.17	Unclassified
148223359 28436792	*Xenopus laevis*	Atp5b protein (ATP synthase H+transporting mitochondrial F1 complex b)/ATP synthase subunit beta/MGC53838	DR(2)		(−)1.20	ATP and nucleotide binding; hydrolase and hydrogen ion transmembrane transporter activity
148223147 51258410	*Xenopus laevis*	An2 (ATP synthase subunit alpha)/LOC397732 protein/MGC84051	DR(3)		(−)1.17	ATP and nucleotide binding; hydrolase and hydrogen ion transmembrane transporter activity
42490818 148237866	*Mus musculus* *Xenopus laevis*	[f]Ubb (ubiquitin B) hypothetical protein LOC779345/UbC/MGC53081	UR(2)		(+)1.34	Protein binding and modification
56606037 6006270	*Mus Musculus* *Xenopus laevis*	[f]SET (hypothetical protein LOC434632)/ TAF1b2 (template activating factor 1b2)	UR(2)		(+)1.22	DNA binding
140832784 156718016	*Xenopus tropicalis*	[f]LOC100125195 protein/Unknown (protein for MGC:122680)	UR(2)		(+)1.25	Nucleic acid synthesis
27503841 82242628	*Xenopus laevis*	Nsep1 protein (nuclease sensitive element binding protein 1)/Y-box-binding protein/ MGC52606	UR(3)		(+)1.26	DNA and protein binding; receptor and transcription factor activity
70778734 147901554	*Danio rerio* *Xenopus laevis*	[f]Atp1a3b (ATPase, Na+/K+transporting, alpha 3 beta)/Atp1a3-prov protein/MGC52867	DR(3)		(−)1.19	ATP and nucleotide binding; transmembrane transporter cation hydrolase activity
74220042 66911182	*Mus Musculus* *Xenopus laevis*	[f]Tuba1 (tubulin alpha 1a chain; unnamed protein product)	DR(3)		(−)1.26	Structural molecule activity; nucleotide and GTP binding
148233446 27370852	*Xenopus laevis*	Marcks-prov (myristoylated alanine rich protein kinase C substrate/MGC52672)	UR(2)		(+)1.34	Calmodulin binding
148232220 138531	*Xenopus laevis*	Vim 1 (vimentin)/MGC83389	UR(2)		(+)1.18	Structural molecule activity; protein binding
49037474 49037471	*Homo sapiens* *Xenopus laevis*	[f]CALM (calmodulin phosphorylase kinase, delta)/CaM (calmodulin 1/2)	UR(2)		(+)1.23	Protein and N-terminal myristoylation domain binding; calcium ion binding; signal transduction
148223251 147905738	*Xenopus laevis*	G protein alpha subunit (guanine nucleotide binding protein alpha)/LOC398037	DR(2)		(−)1.18	Nucleotide and GTP binding; signal transduction, grow factor and receptor activity
55742372 27503247	*Xenopus tropicalis* *Xenopus laevis*	[f]Sfrs1 (splicing factor arginine/serine-rich 1; fragment)/Sfrs1 protein	UR(2)		(+)1.11	Nucleic acid binding
34784586	*Xenopus laevis*	Non-muscle Tropomyosin (Tm-4)/MGC68438	UR(2)		(+)1.14	Protein, metal ion and actin binding
148226106 401234	*Xenopus laevis*	Tmsb4 (thymosin beta 4)	UR(2)		(+)1.12	Actin and protein binding
147904551 56269214	*Xenopus laevis*	LOC496060 protein/fabp7		DR(3)/DR(3)	(−)1.19/1.26	Fatty-acid binding; transporter activity
148236456 32450575	*Xenopus laevis*	[g]Ptma protein (prothymosin alpha-a)/MGC64300		NC/UR(2)	NC/(+)1.28	Zinc ion binding; enzyme inhibitor activity

[c]Average fold change for proteins in iTRAQ experiments was calculated from the individual protein expression ratios relative to controls for at least two T4 inhibitors.
[g]Response variability for Ptma (12.3 kDa, pI 3.76) is unclear, but maybe related to LC–MS under-sampling or its low pI (which limits the number of arginines and lysines available for tryptic digestion).
[h]MGC84072 and Hypothetical LOC734877 are brain acid soluble proteins (BASP1). Specifically, the BASP1 are neuron enriched Ca2+-dependent calmodulin-binding proteins of unknown function.

replicates from a combined sample. Assessment of *i*TRAQ ratios for individual control and MET-treated pools labeled against the corresponding combined samples (data not shown), and the high reproducibility observed for individual sample pools analyzed in replicate by 2D PAGE (Fig. 1) helped to substantiate this assumption.

4. Discussion

The molecular status of a cell or tissue can be defined by the inventories and abundances of genes, proteins, and metabolites. Because 'omic' technologies measure responses at different levels of biological organization, they provide diverse insights into the biochemical and molecular status of an organism. Molecular profiling with 'omic' techniques can be used as a diagnostic tool to determine whether toxicological effects are mediated by (direct responses) or associated with (compensatory responses) changes in the molecular status of cells and tissues. Molecular profiling may also facilitate elucidation of toxicity mechanisms using indicators of cell function at the molecular level. As part of a larger study, we specifically examined both the protein expression profiles produced by T4 synthesis inhibitors in the *X. laevis* tadpole brain, and the intrinsic limitations involved in the characterization of the anuran tadpole brain proteome. We then used this information as the basis to propose that distinctive protein profiles obtained in the intact brain could be used as potential diagnostic indicators of chemical effect and HPT disruption for selected classes of compounds. Proteomic assessment

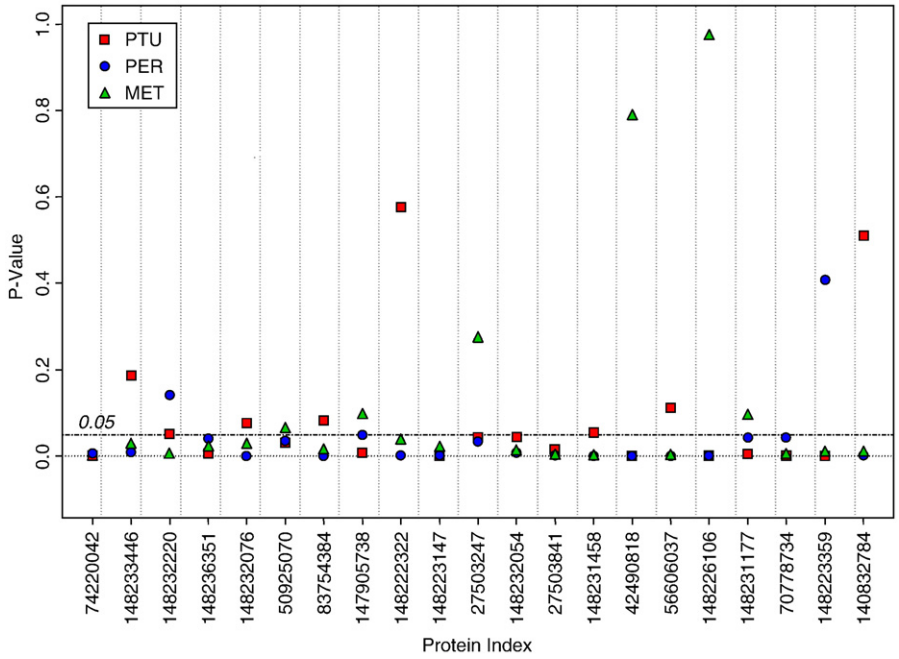

Fig. 2. *p*-value associated with *i*TRAQ ratio and accession number for proteins differentially expressed at 96 h by a minimum of two T4 inhibitors (PTU—6-propylthiouracil; PER—perchlorate; MET— methimazole). Three *p*-values are displayed for each protein corresponding to 3 chemical exposures. Plot shows that >75% of all *p*-values are significant (<0.05). Six of the proteins show significant changes after treatment with all three chemicals as follows, 1) decrease in relative abundance levels: Hsp90b (148232054), An2/LOC397732 (148223147), Atp1a3 (70778734) and Tuba1 (74220042); 2) increase in relative abundance levels: Tpi (148236351) and Nsep1 (27503841). Three proteins differentially expressed by two of the chemicals showed values at the lower limit of the 95% confidence interval (CI) for the remaining T4 inhibitor but were not reported as altered by all chemicals. The proteins were identified as Xtp (50925070), MGC132184/LOC734877 (148232076), and Stmn1 (148231458). Most likely, slightly higher than 0.05 *p*-values for protein ratios accounted for the observed values at the lower limits of the CI. For protein full name see Table 2.

of *X. laevis* brain from larvae presented both common and distinctive challenges. The challenges included: 1) unknown expression levels for low abundant proteins (e.g. <1000 copies/cell), 2) the analysis of pituitary-containing brain, 3) the requirement of a large number of individuals for adequate amounts of tissue and protein, 4) the lack of an annotated protein database required for protein identification, and 5) the number of individual samples required per replica. Since the pituitary gland is less than 1% of the intact brain, it was not chosen as the target tissue. Still, the greatest challenge continued to be the harvesting of the brain for a single multi-chemical, multi-exposure time experiment. For protein identification, the lack of a complete annotated genome sequence required implementation of homology-

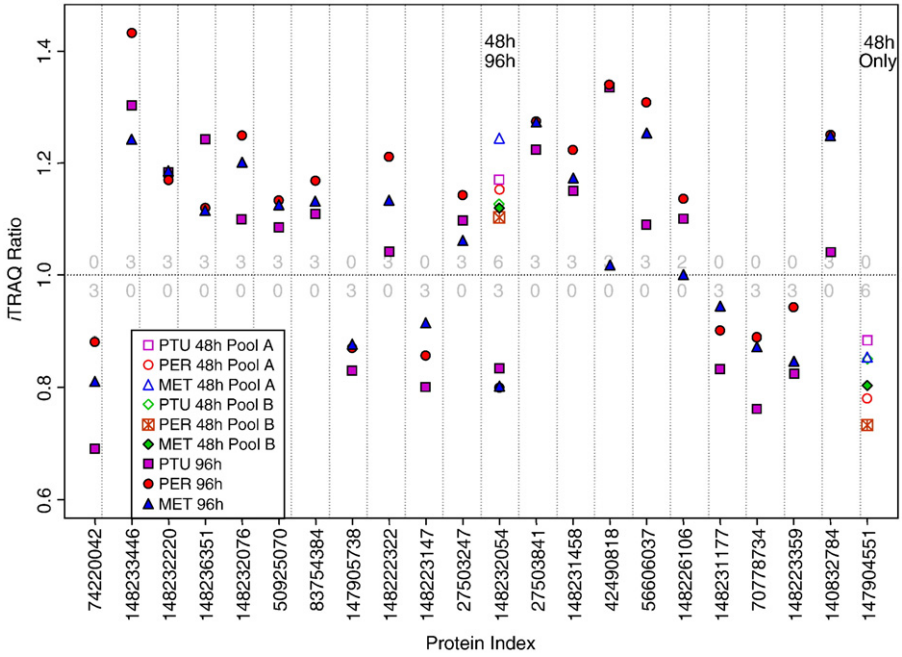

Fig. 3. Distribution of *i*TRAQ ratios and accession numbers for proteins differentially expressed by a minimum of two T4 inhibitors at 96 and 48 h. Three ratios are shown per protein, per exposure time. *p*-values for the plotted ratios are presented in the Supplemental information section. Plot displays the number of ratios below and above unity for each protein and confirms that significant ratios differ from unity for expressed proteins in brain extracts. Hsp90b (148232054) shows upregulation and downregulation at 48 and 96 h of exposure respectively, an example of a brain protein expression response that requires further investigation.

Table 3
Associated or potential regulatory pathways for differentially expressed *Xenopus laevis* brain proteins.

Abbreviated protein name from Tables 1 and 2	Associated or potential regulatory pathway (from PIR/KEGG)	Selected links
Ckb	Arginine and proline metabolism [PATH:xla00330] Metabolic [PATH:xla01100]	PATH:xla00330
Hsp90beta	Progesterone-mediated oocyte maturation [PATH:xla04914]/NOD-like receptor signaling [PATH:xla04621]	PATH:xla04914
Stmn1/Xtp/Hsc70	MAPK signaling [PATH:xla04010]	PATH:xla04010
Atp5b/An2/Uqcrc1	Oxidative phosphorylation [PATH:xla00190]	PATH:xla00190
Tpi	Inositol phosphate metabolism [PATH:xla00562]/Fructose and mannose metabolism [PATH:xla00051]/Glycolysis/Gluconeogenesis [PATH:xla00010]	PATH:xla00562
Aldolase C	Glycolysis/Gluconeogenesis [PATH:xla00010]/Pentose phosphate[PATH:xla00030]/ Metabolic [PATH:xla01100]	PATH:xla00030
eno1	Glycolysis/Gluconeogenesis [PATH:xla00010]/Metabolic [PATH:xla01100]/RNA degradation [PATH:xla03018]	PATH:xla00010
CaM	Calcium signaling [PATH:xla04020]/Phosphatidylinositol signaling [PATH:xla04070]	PATH:xla04020
SNAP-25	SNARE interactions in vesicular transport [PATH:xla04130]	PATH:xla04130
Tubb5/Tuba1	Gap junction [PATH:xla04540]	PATH:xla04540
Hnrpk/LOC397751/MGC84000(G isoform beta)	Spliceosome [PATH:xla03040]	PATH:xla03040
G isoform alpha	Melanogenesis [PATH:xla04916]/Calcium signaling [PATH:xla04020]/Gap junction [PATH:xla04540]	PATH:xla04916
LOC496060/Ubc	Peroxisome proliferator-activated receptors (PPAR) signaling [PATH:xla03320]	PATH:xla03320]
Flot1c	Insulin signaling pathway [PATH:xla04910]	PATH:xla04910]
Atp1a3	Cardiac muscle contraction [PATH:xla04260]/Potential: Oxidative phosphorylation/	PATH:xla04260
Xac1/Tmsb4	Regulation of actin cytoskeleton [PATH:xla04810]/Potential: Axon guidance	PATH:xla04810
20S proteasome a5	Not specified for X. laevis/Potential: Proteasome	PATH: ath03050
Vcp/Dpys13 (DRP3a)/LOC494650 (DRP3b)	Not specified for X. laevis/Potential: Purine metabolism	PATH: pic00230
Alpha fodrin (spectrin)/Nsep1	Not specified for X. laevis/Potential: Tight junction	PATH: mmu04530
14–3–3 protein z	Not specified for X. laevis/Potential: Cell cycle	PATH: bta04110
Hspa5	Not specified for X. laevis/Potential: RNA degradation	PATH: ana03018
Mdh2a	Not specified for X. laevis/Potential: Glycolysis/Gluconeogenesis and pyruvate metabolism	PATH: ban00620
Marcks/Vim1/XNIF/LOC398459/Tm-4	Not specified for X. laevis	
Sfrs1/Ddah1/Ptma/Cct5/MGC81949 (Cct6a)/Capzb/Fubp1/MGC132184/ MGC84072/TAF1b2/LOC100125195	Unknown	

based search strategies and utilization of large nrNCBI database subsets with non-*Xenopus* proteins.

Although thyrostatics with different mechanism of action were used in our experiments (PTU, PER and MET; Degitz et al., 2005), the net effect of each one (mode of action) is an ultimate decrease in T4 production in the thyroid gland and subsequent depletion of T4 from the serum (Tietge et al., 2010). Therefore we hypothesized that physiological changes in the brain are reflected in the proteome, and that xenobiotics triggering T4 synthesis inhibition will also produce analogous brain protein profiles. Previous studies using a combination of cDNA array analysis and QPCR (Helbing et al., 2007a,b), demonstrated that the anuran brain is sensitive to gene expression alteration by PTU, PER, and MET with the least reliable responses obtained at 24 h. Our protein expression results showed a good correlation with these genomic observations. In addition, while PER played the most important role in the expression of gene transcripts associated with neural development and function, our data demonstrated that proteins associated to processes such as neurogenesis (LOC734877), regulation of synapse organization (alpha fodrin), and regulation of growth rate (Cct5; Cct6a) were in fact differentially regulated by all chemicals approximately in the same way. Helbing and co-authors also noticed that PTU responses tended to group more with PER than with MET at 48 and 96 h, a feature that was also confirmed for some of the regulated proteins in our work. A direct effect of the chemicals on the brain tissue has been provided as a potential explanation for this observation. Genomic data showed the highest number of altered gene transcripts encoding proteins associated with transcription processes, hormonal regulation, protein processing, structural function, cell growth control, metabolism and signal transduction. In our study, proteins showing the greatest alteration by chemical effects at both exposure times were also associated with metabolic processes (Tpi, Ckb, DRP3, LOC494650, LOC496060), neurotransmission and signal transduction (SNAP-25, CaM), transcription activity, nucleic acid/protein binding and synthesis (14–3–3 protein Z, Xac1, LOC397751, Hnrpk, Flot1c, Vcp, Fubp1, Hsp90b,UbC, Atp5b, TAF1b, LOC100125195, Tm-4, Nsep1) and calmodulin binding (Marcks). Structure modifications such as glycosylation and/or relative lower abundance in total brain lysates at short exposure periods most likely account for the reduced identification of expressed proteins associated with hormonal regulation by either peptide labeling or 2D PAGE. Common molecular functions associated to expressed brain genes and proteins included protein, nucleic acid, ATP and tubulin/actin binding, hydrolase/lyase/catalase/transferase/ATPase activity, signal transduction and receptor/transcription factor activity. The bulk of the proteins identified from gel and *i*TRAQ analyses support the activation of the same type of responses as a result of larvae exposure to the three thyrostatics. Similarly, comparison of differential protein and gene expression data for the developing anuran brain also suggests the activation of the same type of responses after chemical exposure. However, the correlation between these protein/gene regulation changes and adverse responses at higher levels of biological organization remains largely unknown, and is the current focus of our investigation. In addition, a limited number of proteins were differentially regulated by two or all chemicals at both 48 and 96 h. Limited protein expression is attributed to the comparatively short exposure times selected for this initial experiment and not to the experimental rationale. In fact, a recent investigation of the magnitude of temporal responses for several thyroid-related endpoints in larval *X. laevis* exposed to the same thyrostatics (circulating T4, follicular cell hyperplasia and hypertrophy, diffuse thyroidal hypertrophy, colloid depletion, follicular enlargement, thyroid cell numbers and thyroidal MIT, DIT and T4; see Tietge et al., 2010) suggests that a higher level of anuran HPT compensatory responses occur at or after 144 h of exposure. Nevertheless, brain gene and

protein differential expression patterns, the regulation of pituitary TSH (unpublished data), and some of the reported changes in thyroid endpoints at 96 h exposure (e.g., thyroid histology and thyroidal T4) suggest that alterations in brain molecular and cellular status as well as compensatory processes are activated as early as 48 h of chemical exposure. Therefore, signature protein expression profiles produced by T4 inhibitors at 48 and 96 h were characterized within the experimental conditions applied, and regulation information related to chemical effect in the pro-metamorphic anuran brain was obtained for further diagnostic applications.

Recent studies have suggested that the HPT axis, especially its hypothalamic control is not highly conserved among vertebrates (Bernier et al., 2009; De Groef et al., 2006). Adding to this uncertainty, the anuran brain proteome composition and its resemblance to higher vertebrates have not been well assessed. Typically, 2D PAGE analysis of total brain samples such as unfractionated human brain extracts has resulted in the detection of a ubiquitous group of proteins from brain tissue that includes heat shock (Hsp), Hsc, Hsp70, Hspa5 (GRP78), tubulin chains, and house-keeping enzymes like eno1 and ATP synthase (Garbis et al., 2005; Fountoulakis, 2004). Most of the proteins in brain samples have been identified in other tissues. For example, Hsc and Hspa5 are found in mouse and rat liver proteomes, and are also considered internal markers (positive controls) of a successful identification process for protein batch analysis. Our 2D PAGE data provided evidence for the presence and regulation of Tubb5 and Tubb2 chains, eno1, Hsc70, and Hspa5 in all *X. laevis* brain samples. In addition, *i*TRAQ results validated the identity and expression of Hsp90b, An2 and Atp5b in the brain. All of these proteins showed decreased relative abundance by T4 inhibitors at 48 or 96 h, indicating that actual alterations in protein regulation exist in the samples. Interestingly, an overall downregulation response was observed for brain genes affected by all three chemicals at the same exposure times. Thus, data obtained by both techniques confirmed the presence of a number of conserved proteins in the anuran brain, and also suggest an important role for ubiquitous proteins as targets for the chemical effect of T4 inhibitors. In general, the information derived from frequently detected gene products is of limited value to the search for potential drug targets and biological markers. However, due to the nature and composition of the brain proteome and the study outcomes, we propose that for the assessment of brain protein expression in anuran species, screening for changes in relative abundance of both ubiquitous and less-frequently detected proteins as a result of exposure to target endocrine disrupters would provide a more appropriate benchmark to facilitate the: 1) understanding of HPT responses to chemical insult, 2) potential adverse outcomes associated to exposure and, 3) search for potential diagnostic indicators of endocrine disruption.

A key challenge in the post-genomic era is the identification of the function(s) of all the molecules in a given organism (Skolnick and Brilinski, 2009; Schilling et al., 2000). The use of both gel-based and stable isotope labeling in combination with MS technologies and toxicogenomic tools has been suggested as a mechanism to advance the understanding of molecular cascades activated or disrupted by chemical effect when assessing the proteome of both model and non-model species (Martyniuk et al., 2009). Due to the presence of conserved proteins in the anuran brain, we speculate that even though the specific hypothalamic hormones that stimulate the release of TSH from the pituitary may differ between mammals and other vertebrates, it is likely that the overall response of the brain to T4 synthesis inhibition due to exposure to thyrostatics would be fairly well-conserved, and that compensatory responses reflected as regulation changes in *X. laevis* brain proteins and further activation of associated regulatory pathways will be similar among vertebrates. To obtain some insight into the potential effect of T4 inhibitors on higher order cellular function, we aimed at the identification of regulatory pathways associated with differentially expressed *X. laevis* brain proteins. For this purpose, we searched information stored in the KEGG PATHWAY database. We learned that regulatory pathways to model cellular processes are specified only for approximately half of the *X. laevis* expressed proteins assessed. For example, Stmn1, Xtp, and Hsc70 were grouped in the mitogen-activated protein kinase (MAPK) cascade pathway. These findings suggest a potential link between T4 synthesis inhibition effects in the brain proteome and biological responses such as cell proliferation, differentiation and signaling. Similarly, Xac1 and Tmsb4 were grouped in a pathway regulating processes such as actin cytoskeleton and axon guidance in higher vertebrates, a sign of a potential adverse effect of endocrine disrupters on key stages of the neuronal network formation. Further examination of previously reported genomic data at 48 and 96 h (Helbing et al., 2007a,b), showed alteration of various gene transcripts encoding proteins associated with the same regulatory pathways as reported for brain proteins (Table 3) including: Progesterone-mediated oocyte maturation (c-Mos/Maskin/RPD3); oxidative phosphorylation (SERCA1), regulation of actin cytoskeleton (C-Src kinase) and cell cycle (Cdc21). The identification of common cellular pathways associated with gene and protein regulation in *X. laevis* brain provided support for the conviction that these pathways could be thyroid hormone-mediated in anuran and other vertebrate species. Overall, the collection of molecular functions and biological processes assigned to *X. laevis* larvae brain expressed proteins, as well as the regulatory pathways found associated with these proteins suggest the potential activation of a collection of metabolic, bioenergetic, cell signaling and transcription/translation compensatory processes in the anuran brain as an early response to T4 synthesis inhibition. These observations are being currently used to complement phenotypic changes associated to T4 synthesis inhibition compensation in the anuran tadpole. Finally, some protein regulation responses detected in the anuran brain were not well understood. Specific examples are the reversed expression of both Hsp90b and guanine nucleotide binding protein alpha and beta (MGC84000) isoforms at different time points. Lack of greater information on the underlying dynamic changes occurring in the brain at any timepoint, proteolytic cleavage, and post-translational modifications are among potential explanations for these observations.

We conclude that additional research at extended exposure times is necessary to better assess both the persistence/significance of various protein expression responses observed in the tadpole brain, and the biological processes/networks affected by protein regulation. We also conclude that despite a lack of highly comparable quantitative responses between both proteomic technologies, 2D PAGE and *i*TRAQ are good complementary techniques for assessing the effects of thyroid active chemicals in the developing anuran brain as well as in other tissues critical to the vertebrate HPT compensatory response to T4 synthesis inhibition (e.g., characterization of a *X. laevis* partial pituitary proteome and TSH regulation assessment from intact pituitaries at 48 and 96 h to complement brain protein expression profiles; Serrano et al., unpublished results). Because of the capability of separation by pI and mass, 2D PAGE facilitated the identification of protein fragments in comparison with peptide labeling. However, we also confirmed that for small amounts of anuran brain, *i*TRAQ LC–MS/MS is more sensitive, facilitates analysis of hard-to-characterize acidic/basic, low/high MW, low abundant and less soluble proteins, and provides a broader coverage than SDS PAGE (Martyniuk and Denslow, in press). *i*TRAQ labeling approaches have been validated by various methods (Unwin et al., 2005; Cong et al., 2006, Wiese et al., 2007), and applied to the assessment of both prokaryotic and eukaryotic samples including to the proteomic analysis of the anuran tail fin during metamorphosis (Domansky and Helbing, 2007). However to the best of our knowledge, this is the first report of the application of proteomic technologies such as *i*TRAQ peptide labeling and gel electrophoresis to characterize and document brain proteins from an anuran species after *in vivo* exposures to endocrine disrupters. In the next step of our investigation, proteins showing distinctive responses

were considered for further assessment as candidates for diagnosis of T4 inhibition. Specifically, protein candidate selection relied upon the identification and validation of characteristic expression profiles with the proteomic technologies here described. Examination of differential regulation data provided by proteomic tools was then used to distinguish suitable potential protein candidates. Examples include Tpi (a brain and pituitary carbohydrate metabolism enzyme), and SNAP-25 (a brain and pituitary highly conserved t-SNARE complex protein). The 96 h upregulation of SNAP-25 is of particular interest as upregulation in the adenohypophyses of thyroidectomized rats, reversal of effect by T4 administration, and downregulation in the adrenal gland by T4 have been reported for this protein (Quintanar and Salinas, 2002, Zhang et al., 2008). A detailed evaluation of the potential of amphibian brain protein profiles as screening/diagnostic tests of TH synthesis inhibition activity for endocrine xenobiotics is presented in a complementary, follow-up manuscript. Overall, we intend to support the development of an anuran HPT model that integrates data from various levels of biological organization into a system that would facilitate understanding of T4 inhibition in aquatic species. Such a system would provide sensitive diagnostic tools and a potential mechanism to predict the adverse effects of endocrine disrupters to relevant organisms. It is expected that molecular profiling information correlated to chemical exposure like the one presented in this report will facilitate the development of additional *in vitro* and short-term *in vivo* assays needed to support hypothesis-based risk assessment in toxicology. The need to understand molecular-level events associated with toxicity pathways and adverse outcomes would also promote further integration of 'omic'-based approaches into chemical screening and assessment programs. Furthermore, the understanding of molecular- and cellular-level responses associated with the adverse effects of endocrine disrupters to aquatic life would contribute to the advancement of methods for species extrapolation. Interpretation of interspecies homology and comparative toxicity would also benefit from molecular level diagnostic endpoints. Finally, correlation of differential protein profiling information to cellular- and organism-level endpoints will contribute to the development of a rapid, cost-effective, non-mammalian screening assay for thyroid axis-disrupting chemicals.

Acknowledgments

Authors want to thank Benji Hanson (Computer Science Corporation, Duluth, MN) and Thomas McGowan (University of MN, St Paul) for very valuable bioinformatics, statistical, and graphics support. We are also grateful to Drs. Daniel Villeneuve, Michael Hornung, Witold Winnik, David Bencic (USEPA), and Nancy Denslow (University of Florida) for the critical review of this manuscript. Research was supported by ACC CRADA (Endocrine Disrupters; 405SA8), and in part by the USEPA-ORD Computational Toxicology Program. The authors recognize the Center for Mass Spectrometry and Proteomics at the University of Minnesota and various supporting agencies, including the National Science Foundation for Major Research Instrumentation grants 9871237 and NSF-DBI-0215759 used to purchase the instruments described in this study.

Appendix A. Supplementary data

Supplementary data associated with this article can be found, in the online version, at doi:10.1016/j.cbd.2010.03.007.

References

Albertsson, E., Kling, P., Gunnarsson, L., Larsson, D.G., Forlin, L., 2007. Proteomic analyses indicate induction of hepatic carbonyl reductase/20ß- hydroxysteroid dehydrogenase B in rainbow trout exposed top sewage effluent. Ecotoxicol. Environ. Safety 68, 33–39.

Ankley, G.T., Miracle, A.N., Perkins, E.J., 2008. Toxicogenomics in ecological risk assessments: regulatory context, technical background and workshop overview. In: Ankley, G.T., Miracle, A.N. (Eds.), Genomics in Regulatory Ecotoxicology, Chapter 1. Taylor and Francis-SETAC Press, pp. 5–18.

Ankley, G.T., Bennett, R., Erickson, R.J., Hoff, D.J., Hornung, M.W., Johnson, R.D., Mount, D.R., Nichols, J.W., Russom, C.L., Schmieder, P.K., Serrano, J., Tietge, J.E., Villeneuve, D.L., 2010. Adverse outcome pathways: a conceptual framework to support ecotoxicology research and risk assessment. Environ. Toxicol. Chem. 29, 730–741.

APHA (American Public Health Association), American Water Works Association, Water Environment Foundation, 1992. Standard methods for the examination of water and wastewater, 18th ed. Washington, DC.

Balgley, B.M., Laudeman, T., 2007. Comparative evaluation of tandem MS search algorithms using a target-decoy search strategy. Mol. Cell Proteomics 6, 1599–1608.

Bernier, N.J., Flik, G., Klaren, P.H.M., 2009. Regulation and contribution of the corticotropic, melanotropic and thyrotropic axes to the stress response in fishes. In: Bernier, N.J., Van Der Kraak, G., Farrell, A.P., Brauner, C.J. (Eds.), Fish Physiol., 28, pp. 235–311.

Borgert, C.J., Quill, T.F., McCarty, L.S., Mason, A.M., 2004. Can mode of action predict mixture toxicity for risk assessment? Toxicol. Appl. Pharmacol. 201, 85–96.

Bradley, B.P., Schrader, E.A., Kimmel, D.G., Meiller, J.C., 2003. Protein expression signatures: an application of proteomics. Mar. Environ. Res. 54, 373–377.

Brown, D.D., Wang, Z., Furlow, J.D., Kanamori, A., Schwartzman, R.A., Remo, B.F., Pinder, A., 1996. The thyroid hormone-induced tail resorption program during *Xenopus laevis* metamorphosis. Proc. Natl Acad. Sci. U. S. A. 93, 1924–1929.

Choe, L., Aggawarl, K., Franck, Z., Lee, K.H., 2005. A comparison of the consistency of proteome quantitation using two-dimensional electrophoresis and shotgun isobaric tagging in *E. coli* cells. Electrophoresis 26, 2437–2449.

Committee on toxicity testing and assessment of environmental agents, N.R.C., 2007. Toxicity Testing in the 21st Century: a Vision and a Strategy. National Academies Press.

Cong, Y.S., Fang, E., Wang, E., 2006. Simultaneous proteomic profiling of four different growth states of human fibroblasts using amine-reactive isobaric tagging reagents and mass spectrometry. Mech. Ageing Dev. 127, 332–343.

Craig, R., Beavis, R.C., 2004. Tandem: matching proteins with tandem mass spectra. Bioinformatics 20, 1466–1467.

Daston, G.P., Miracle, A.N., Perkins, E.J., Ankley, G.T., 2008. Toxicotranscriptomics in ecological risk assessments: regulatory context, technical background and workshop overview. In: Ankley, G.T., Miracle, A.N. (Eds.), Transcriptomics in Regulatory Ecotoxicology, Chapter 7. Taylor and Francis-SETAC Press, pp. 151–156.

De Groef, B., Van der Geyten, S., Darras, V.M., Kühn, E.R., 2006. Role of corticotropin-releasing hormone as a thyrotropin-releasing factor in non-mammalian vertebrates. Gen. Comp. Endocrinol. 146, 62–68.

Degitz, S.J., Holcombe, G.W., Flynn, K.M., Kosian, P.A., Korte, J.J., Tietge, J.E., 2005. Progress towards development of an amphibian-based thyroid screening assay using *Xenopus laevis*. Organismal and thyroidal responses to the model compounds 6-propylthiouracil, methimazole, and thyroxine. Toxicol. Sci. 87, 353–364.

Domansky, D., Helbing, C.C., 2007. Analysis of the *Rana catesbeiana* tadpole tail fin proteome and phosphoproteome during T3-induced apoptosis: identification of a novel type I keratin. BMC Dev. Biol. 7, 94–99.

Edwards, S.W., Preston, R.J., 2008. Systems biology and mode of action based risk assessment. Toxicol. Sci. 106 (2), 312–318.

Ekman, D., Teng, Q., Jensen, K., Martinovic, D., Ankley, G., Collette, T., 2007. NMR analysis of male fathead minnow urinary metabolites: a potential approach for studying impacts of chemical exposures. Aquat. Toxicol. 85, 104–112.

Elias, J.E., Haas, W., Faherty, B.K., Gygi, S.P., 2005. Comparative evaluation of mass spectrometry platforms used in large scale proteomic investigations. Nat. Methods 2, 667–675.

Ernoult, E., Gamellin, E., Guette, C., 2008. Improved proteome coverage by using iTRAQ labelling and peptide OFFGEL fractionation. Proteome Sci. 6 (27), 1–13.

Fountoulakis, M., 2004. Application of proteomics technologies in the investigation of the brain. Mass Spectrom. Rev. 23, 231–258.

Garbis, S., Lubec, G., Fountoulakis, M., 2005. Limitations of current proteomics technologies. J. Chromatogr. A 1077, 1–18.

Garcia-Reyero, N., Villeneuve, D.L., Kroll, K.J., Liu, L., Orlando, E.F., Watanabe, K.H., Sepulveda, M.S., Ankley, G.T., Denslow, N.D., 2009. Expression signatures for a model androgen and antiandrogen in the fathead minnow. Environ. Sci. Technol. 43, 2614–2619.

Gasser, P.J., Orchinick, M., 2006. Vasopressin-induced translocation and proteolysis of protein kinase Cα in an amphibian brain: modulation by corticosterone. Brain Res. 1134, 18–26.

Gatlin, C.L., Kleemann, G.R., Hays, L.G., Link, A.J., Yates, J.R., 1998. Protein identification at the low femtomole level from silver-stained gels using a new fritless electrospray interface for liquid chromatography-microspray and nanospray mass spectrometry. Anal. Biochem. 263, 93–101.

Grim, K.C., Wolfe, M., Braunbeck, T., Iguchi, T., Tooi, O., Touart, L., Wolf, D., Tietge, J., 2009. Thyroid histopathology assessments for the amphibian metamorphosis assay to detect thyroid-active substances. Toxicol. Pathol. 37, 415–424.

Helbing, C.C., Bailey, C.M., Ji, L., Gunderson, M.P., Zhang, F., Skirrow, R.C., Lesperance, M., Holcombe, G.W., Kosian, P.A., Tietge, J.E., Korte, J.J., Degitz, S.J., 2007a. Identification of gene expression indicators for thyroid axis disruption in a *Xenopus laevis* metamorphosis screening assay. Part 1: effects on the brain. Aquat. Toxicol. 82, 227–241.

Helbing, C.C., Bailey, C.M., Ji, L., Zhang, F., Holcombe, G.W., Kosian, P.A., Tietge, J.E., Korte, J.J., Degitz, S.J., 2007b. Identification of gene expression indicators for thyroid axis disruption in a *Xenopus laevis* metamorphosis screening assay. Part 2: effects on the tail and hindlimb. Aquat. Toxicol. 82, 215–226.

Hemmer, M.J., Cripe, G.M., Hemmer, B.L., Goodman, L.R., Salinas, K.A., Fournie, J.W., Walker, C.C., 2008. Comparison of estrogen-responsive plasma protein biomarkers and reproductive endpoints in sheepshead minnows exposed to 17B-Trenbolone. Aquat. Toxicol. 88, 128–136.

Issaq, H.J., Chan, K.C., Conrads, T.P., Veenstra, T.D., 2005. Multidimensional separation of peptides for effective proteomic analysis. J. Chromatogr. B 817, 35–47.

Jackson, P.E., Gokhale, S., Streib, T., Rohrer, J.S., Pohl, C.A., 2000. Improved method for the determination of trace perchlorate in ground and drinking waters by ion chromatography. J. Chromatogr. A 888, 151–158.
Johns, S.M., Kane, M.D., Denslow, N.D., Watanabe, K.H., Villeneuve, D.L., Ankley, G.T., Sepulveda, M.S., 2009. Characterization of ontogenic changes in gene expression in the fathead minnow. Environ. Toxicol. Chem. 28, 873–880.
Kanehisa, M., Goto, S., 2000. KEGG: Kyoto encyclopedia of genes and genomes. Nucleic Acids Res. 28 (1), 127–130.
Kapphahn, R.J., Ethen, C.M., Peters, E.A., Higgins, L., Ferrington, D.A., 2003. Modified alpha A crystallin in the retina: altered expression and truncation with aging. Biochemistry 42, 15310–15325.
Kassie, F., Anderson, L.B., Higgins, L., Pan, Y., Matise, I., Negia, M., Upadhyaya, P., Wang, M., Hech, S.S., 2008. Chemopreventive agents modulate the protein expression profile of 4-(methylnitrosamino)-1-(3-pyridyl)-1-butanone plus benzo[a]pyrene-induced lung tumors in A/J mice. Carcinogenesis 29, 610–619.
Keller, A., Nesvizhskii, E., Aebersold, R., 2002. Empirical statistical model to estimate the accuracy of peptide identifications made by MS/MS and database search. Anal. Chem. 74, 5383–5392.
Kling, P., Norman, A., Andersson, P.L., Forlin, L., 2008. Gender-specific proteomic responses in zebrafish liver following exposure to a selected mixture of brominated flame retardants. Ecotoxicol. Environ. Safety 71, 319–327.
Koulman, A., Woffendin, G., Narayana, V.K., Welchman, H., Crone, C., Volmer, D.A., 2009. High-resolution extracted ion chromatography, a new tool for metabolomics and lipidomics using a second generation orbitrap mass spectrometer. Rapid Commun. Mass Spectrom. 23, 1411–1418.
Lin, W.-T., Hung, W.-N., Yian, Y.-H., Wu, K.-P., Han, C.-L., Chen, Y.-R., Chen, Y.-J., Sung, T.-Y., Hsu, W.-L., 2006. Multi-Q: a fully automated tool for multiplexed protein quantitation. J. Proteome Res. 5 (9), 2328–2338.
Lopez, J.L., 2006. Two-dimensional electrophoresis in proteome expression analysis. J. Chromatogr. 849, 190–202.
Lund, T.C., Anderson, L.B., McCullar, V., Higgins, L., Yun, G.H., Grzywacz, B., Verneris, M.R., Miller, J.S., 2007. *iTRAQ* is a useful method to screen for membrane-bound proteins differentially expressed in human natural killer cell types. J. Proteome Res. 6 (2), 644–653.
Martyniuk, C.J., Denslow, N.D., in press. Towards functional transcriptomics in fish using quantitative proteomics. Gen. Comp. Endocrinol.
Martyniuk, C.J., Alvarez, S., Villeneuve, D.L., Ankley, G.T., Denslow, N.D., 2009. Quantitaive proteomic profiles of androgen receptor signaling in the liver of fathead minnows. J. Proteome Res. 8, 2186–2220.
Moseley, M.A., Deterding, L.J., Tomer, K.B., Jorgenson, J.W., 1991. Nanoscale packed-capillary liquid chromatography coupled with mass spectrometry using a coaxial continuous-flow fast atom bombardment interface. Anal. Chem. 63, 1467–1473.
Nesvizhskii, A., Aebersold, R., 2005. Interpretation of shotgun proteomics data: the protein inference problem. Mol. Cell. Proteomics 4, 1419–1440.
Nesvizhskii, A.I., Keller, A., Kolker, E., Aebersold, R., 2003. A statistical model for identifying proteins by tandem mass spectrometry. Anal. Chem. 75 (17), 4646–4658.
Nesvizhskii, A.I., Vitek, O., Aebersold, R., 2007. Analysis and validation of proteomic data generated by tandem mass spectrometry. Nat. Methods 4, 787–797.
Nieuwkoop, P.D., Faber, F., 1994. Normal Table of *Xenopus laevis*. Garland, New York.
Pagliato, L., Nonnis, S., Taverna, F., Ronchi, S., Tadeshi, G., 2006. Prion protein from *Xenopus laevis*: overexpression in *Escherichia coli* of the His-tagged protein and production of polyclonal antibodies. Protein Expr. Purif. 46, 489–494.
Perkins, D.N., Pappin, D.C., Creasy, D.M., Cottrell, J.S., 1999. Probability-based protein identification by searching sequence databases using mass spectrometry data. Electrophoresis 20, 3551–3567.
Portman, N., Lacomble, S., Thomas, B., McKean, P.G., Gull, K., 2009. Combining RNA interference mutants and comparative proteomics to identify protein components and dependencies in a eukaryotic flagellum. J. Biol. Chem. 284, 5610–5619.
Quintanar, J.L., Salinas, E., 2002. Effects of hypothyroidism on synaptosomal-associated protein of 25 kDa and synthaxin-1 expression in adenohypophyses of rat. J. Endocrinol. Invest. 25, 754–758.
Ross, P.L., Huang, Y.N., Marchese, J.N., Williamson, B., Parker, K., Hattan, S., Pillai, S., Dey, S., Daniels, S., Martin, S., Barlet-Jones, M., He, F., Jacobson, A., Pappin, D.J., 2004. Multiplexed protein quantitation in *Saccharomyces cerevisiae* using amine-reactive isobaric tagging reagents. Mol. Cell Proteomics 3, 1154–1169.
Salinas, K.A., Hemmer, M.J., Harris, P.S., Walker, C.C., 2008. A simple and rapid matrix-assisted laser desorption/ionization time of flight mass spectrometry method to screen fish plasma samples for estrogen-responsive biomarkers. Environ. Toxicol. Chem. 27, 1175–1183.
Schilling, C.H., Letscher, D., Palsson, B.O., 2000. Theory for the systemic definition of metabolic pathways and their use in interpreting metabolic function from a pathway-oriented perspective. J. Theor. Biol. 203, 229–248.
Shevchenko, A., 1996. Mass spectrometric sequencing of proteins silver-stained polyacrylamide gels. Anal. Chem. 68, 850–858.
Shilov, I.V., Seymour, S.L., Patel, A.A., Loboda, A., Tang, W.H., Keating, S.P., Hunter, C.L., Nuwaysir, L.M., Schaeffer, D.A., 2007. The Paragon algorithm: a next generation search engine that uses sequence temperature values and feature probabilities to identify peptides from tandem mass spectra. Mol. Cell Proteomics 6, 1638–1655.
Skolnick, J., Brilinski, M., 2009. FINDSITE: a combined evolution/structure-based approach to protein function prediction. Brief. Bioinform. 10, 378–391.
Sriyam, S., Tzao, C., Phutrakul, S., Chen, S.-T., 2007. Enhanced detectability in proteome studies. J. Chromatogr. 849, 91–104.
Sveinsdottir, H., Vilhelmsson, O., Gudmunsdottir, A., 2008. Proteome analysis of abundant proteins in two age groups of early Atlantic cod (*Gadus morhua*) larvae. Comp. Biochem. Physiol. D 3, 243–250.
Tietge, J.E., Holcombe, G.W., Flynn, K.M., Kosian, P.A., Korte, J.J., Anderson, L.E., Wolf, D.C., Degitz, S.J., 2005. Metamorphic inhibition of *Xenopus laevis* by sodium perchlorate: effects on development and thyroid histology. Environ. Toxicol. Chem. 24, 926–933.
Tietge, J.E., Hornung, M.W., Holcombe, G.W., Butterworth, B.C., Kosian, P.A., Korte, J.J., Haselman, J.T., Wolf, M., Degitz, S.J., 2010. Early temporal effects of three thyroid hormone synthesis inhibitors in *Xenopus laevis*. Aquatic Toxicol 98, 44–50.
Unwin, R.D., Pierce, A., Watson, R.B., Sternberg, D.W., Whetton, A.D., 2005. Quantitative proteomic analysis using isobaric protein tags enables rapid comparison of changes in transcript and protein levels in transformed cells. Mol. Cell Proteomics 4, 924–935.
Venkateshwar, G.K., Michailidis, G., Strahler, J.R., Kuick, R., Krishnapuram, R., Srirangam, R., Standiford, T.J., Andrews, P., Omenn, G.S., 2009. Temporal quantitative proteomics by iTRAQ 2D-LC–MS/MS and corresponding mRNA expression analysis identify post transcriptional modulation of actin-cytoskeleton regulators during TGF-β-induced epithelial–mesenchymal transition. J. Proteome Res 8, 35–47.
Villeneuve, D., Knoebl, I., Larkin, P., Miracle, Carter B.J., Denslow, D., Ankley, G., 2008. Altered gene expression in brain and liver of female fathead minnows exposed to fadrozole. J. Fish Biol. 72, 2281–2340.
Walker, C.C., Salinas, K.A., Harris, P.S., Vickery, S.S., Hemmer, M.J., 2006. A proteomic (SELDI-TOF-MS) approach to estrogen agonist screening. Toxicol. Sci. 95, 74–81.
Wehr, T., 2007. Quantitative proteomics: available tools and results of a collaborative study. LCGC 25 (10), 1030–1040.
Wiese, S., Reidegeld, K., Meyer, H., Warscheid, B., 2007. Protein labeling by iiTRAQ: a new tool for quantitative mass spectrometry in proteome research. Proteomics 7, 340–350.
Zhang, H.-M., Su, Q., Luo, M., 2008. Thyroid hormone regulates the expression of SNAP-25 during rat brain development. Mol. Cell. Biochem. 307, 169–175.